CHEMISTRY
A EUROPEAN JOURNAL

DOI: 10.1002/chem.200700930

A Quantum Mechanically Guided View of $Mg_{44}Rh_7$

Robert F. Berger, Stephen Lee,* and Roald Hoffmann*[a]

Abstract: We present a new geometric description of $Mg_{44}Rh_7$, a compound with 408 atoms in its cubic unit cell. Using both experimental site preferences and LDA-DFT-calibrated extended Hückel (eH) calculations as guides, we highlight the structural units within $Mg_{44}Rh_7$ that reflect the electron-richness or electron-poorness of each crystallographic site. The units that best account for these site preferences and electron populations are 34- and 25-atom fragments of the Ti_2Ni structure, rather than the variety of clusters often used to describe complicated intermetallic and ionic structures. These Ti_2Ni pieces, located using a systematic search algorithm, fit together in a beautifully intricate network. An examination of this network reveals some surprising geometric features of $Mg_{44}Rh_7$, including a fractal-like arrangement of similar atomic formations on different length scales, geometrically connected to an approximate fivefold symmetry.

Keywords: intermetallic phases · magnesium · rhodium · semiempirical calculations · solid-state structures

Introduction

When chemists think of intermetallic crystal structures, we tend to focus on a few simple structures with just one or two atoms per unit cell. It is indeed true that many intermetallic structures are variants of the body-centered cubic, face-centered cubic, and hexagonal close-packed structures. However, a survey of known crystal structures reveals that a significant fraction of intermetallics have much more complex structures, with anywhere from several hundred to over one thousand atoms per unit cell.[1–4] Given our abiding love affair with simplicity, these complicated structures, if not avoided, are often viewed as a curiosity. They do not generally form a starting point for our understanding of metals, metallic bonding, or metallic crystal structures. However, if nature has chosen them over all other possible arrangements of several hundred atoms, they must carry within them some basic information about which structural features drive an intermetallic compound to exist.

The atomic positions in these complex structures are so varied that in order to even start making sense of them, the curious scientist must search for some description that allows him or her to organize the atoms into simple, recognizable patterns. Pattern seekers often adopt one of several approaches. In a first such approach, complicated structures may be described in terms of constellations of atoms—"clusters" that make the structures easier to visualize and remember. In another approach, complex intermetallics are discussed in terms of their similarities to simpler, better understood structures. And in still a third approach, these structures are described in terms of their coordination polyhedra—the sets of nearest neighbors around each atom.

Each of these modes of pattern recognition can be immensely helpful, at the very least as a geometrical mnemonic device. Geometry is powerful, meaningful, and deep. But there is more to chemistry than geometry, and approaches to understanding a crystal structure must strive to identify the patterns that are chemically meaningful. When dealing with complicated structures, this goal is difficult to accomplish. For example, in the "cluster" approach to intermetallics, the assemblages of atoms discussed are not actually clusters in a chemical sense, because they are not in any way isolated from the rest of the structure. They are simply arbitrary sets of atoms singled out to facilitate visualization of the structure.

In this paper, we use quantum mechanics of the simplest sort to guide our description of a complicated intermetallic structure. Using $Mg_{44}Rh_7$, which crystallizes in the cubic space group $F\bar{4}3m$ (No. 216), as our system of choice, we build up a structural description by drawing from each of

[a] R. F. Berger, Prof. S. Lee, Prof. R. Hoffmann
Department of Chemistry and Chemical Biology
Cornell University, Ithaca, NY 14853-1301 (USA)
Fax: (+1) 607-255-4137
E-mail: sl137@cornell.edu
rh34@cornell.edu

Supporting information for this article is available on the WWW under http://www.chemeurj.org/ or from the author.

the pattern recognition modes mentioned above. Starting with a conventional cluster description of $Mg_{44}Rh_7$, we locate familiar repeating motifs from a simpler structure type throughout the unit cell. From these we build up coordination polyhedra in a new way that suggests an almost fractal character to the structure. The difference from a conventional cluster approach is that by incorporating electronic structure calculations in our geometric description, we emphasize those geometric features that are implicated by quantum mechanics to be important to the stability and bonding of the compound. By constructing a description that is both chemically meaningful and geometrically palatable, one might say we try to have our quantum theory and eat it too. The ultimate goal in this approach is to determine which features allow such beautifully complicated intermetallic structures to exist.

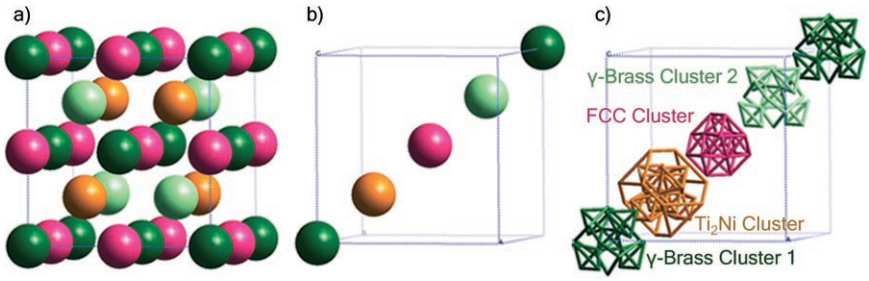

Figure 1. The arrangement of clusters in the $Mg_{44}Rh_7$ structure. a) The four unique clusters are represented by differently colored spheres. Clusters are centered at the high-symmetry points of the crystal, with four copies of each cluster in the cubic unit cell in a face-centered arrangement. b) Clusters are shown along the body diagonal, and c) their identities are revealed.

Results and Discussion

Current understanding of $Mg_{44}Rh_7$: When the crystal structure of $Mg_{44}Rh_7$ was solved by Westin in 1971,[5] it provided solid-state chemists with a puzzle. Since then, a series of well-crafted geometric descriptions have given us several coherent ways of looking at the structure, which has 408 atoms in its cubic unit cell. Samson and Hansen[6] built the $Mg_{44}Rh_7$ structure from icosahedra, pentagonal prisms, and Friauf polyhedra, noting in particular the prevalence of fivefold symmetry. Subsequently, Andersson[7] built the structure from tetrahedra and octahedra, packing them together to form pyrochlore and Keggin units.

Others have described $Mg_{44}Rh_7$ by using the cluster concept, an approach first introduced by Bradley and Jones.[8] The cluster view of $Mg_{44}Rh_7$, shown in Figure 1, describes the structure in terms of a face-centered cubic Bravais lattice of four distinct clusters of atoms. These clusters are centered at the high-symmetry points of the unit cell: (0,0,0), ($^1/_4$,$^1/_4$,$^1/_4$), ($^1/_2$,$^1/_2$,$^1/_2$), and ($^3/_4$,$^3/_4$,$^3/_4$). Several other structures[1] with similarly sized cubic unit cells have also been described in terms of clusters.[9,10] Because the four clusters provide a convenient starting point for our analysis of the $Mg_{44}Rh_7$ structure, we now describe each of these clusters in greater detail.

The clusters in $Mg_{44}Rh_7$: Of the four crystallographically distinct clusters in the $Mg_{44}Rh_7$ structure, two are 26-atom units known as γ-brass clusters. The γ-brass cluster, so named for its presence in Cu_5Zn_8, is most commonly viewed as a set of four nested polyhedra.[8] The cluster has four distinct atomic sites, named for each of these polyhedra, as shown in Figure 2a–d. From the cluster center outward, the four sites are: inner tetrahedron (IT), outer tetrahedron (OT), octahedron (OH), and cubo-octahedron (CO). While these designations make the cluster easier to visualize, the connections shown between atoms are not always as chemically meaningful. For example, the cubo-octahedron connects atoms on the order of 5 Å apart—significantly longer than any reasonable bond length.

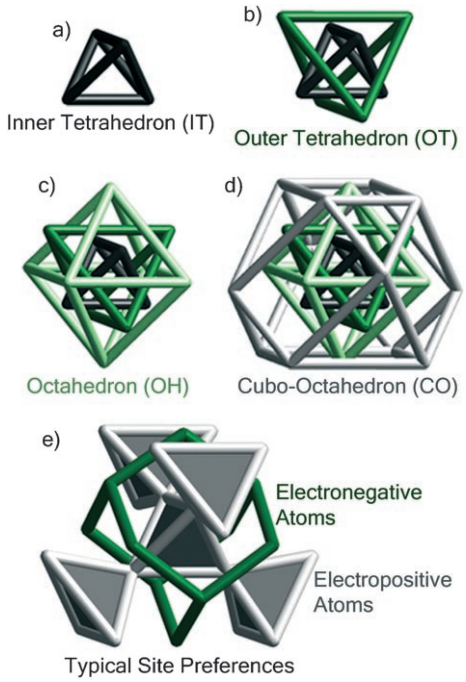

Figure 2. The γ-brass cluster, viewed as four nested polyhedra: a) an inner tetrahedron, b) an outer tetrahedron, c) an octahedron, and d) a cubo-octahedron. e) Alternatively, the cluster can be seen as a tetrahedron of tetrahedra and an adamantane cage.

[1] These structures include $Li_{22}Pb_5$,[11] Na_6Tl,[6] Mg_6Pd,[12] $Cu_{41}Sn_{11}$,[13] $Sm_{11}Cd_{45}$,[14] $Zn_{78}Fe_{22}$,[15] $Li_{22}Si_5$,[16] $Zn_{6.5}(Fe,Ni)$,[17] $Al_{69}Ta_{39}$,[18] $Mg_{29}Ir_4$,[19] $Zn_{20.44}Mo$,[20] $Zn_{21}Pt_5$,[21] and $Li_{13}Na_{29}Ba_{19}$.[22] Each of these compounds crystallizes in space group $F\bar{4}3m$ (No. 216), has between 396 and 488 atoms in its cubic unit cell, and can be described in terms of distinct clusters centered at the high-symmetry points of the crystal.

An alternative view of the γ-brass cluster places together the IT and CO sites in a tetrahedron of tetrahedra, and the OT and OH sites in an adamantane-like cage. This construction, shown in Figure 2e, is more suggestive of the experimental site preferences in many γ-brass variants. In γ-brass itself (Cu_5Zn_8), for example, Zn atoms occupy the IT and CO sites shown in gray, while Cu atoms occupy OT and OH shown in green.[23] More generally, electronic structure calculations have shown that the less electronegative element in a γ-brass variant prefers the IT and CO sites, while the more electronegative element prefers OT and OH.[24]

In addition to the two 26-atom γ-brass clusters, the $Mg_{44}Rh_7$ structure also contains a 34-atom unit known as a Ti_2Ni cluster, so named for its similarity to the Ti_2Ni structure. Once again, the four distinct sites in this cluster can conveniently be classified as nested polyhedra, as shown in Figure 3a–d. The sites are: octahedron (OH), cubo-octahedron[2] (CO), outer tetrahedron (OT), and truncated tetrahedron (TT). This cluster has previously been described as a smaller 22-atom cluster,[9] but for reasons that will become clear soon, we extend it farther. In compounds with the Ti_2Ni structure, experimental site preferences usually place the more electronegative element at the OT site shown in orange.[4] In Ti_2Ni itself, for example, Ni atoms occupy the OT site and Ti atoms occupy the remaining sites.[26] The Ti_2Ni structure, an interlocking network of these Ti_2Ni "clusters," is shown in Figure 3e. A single one of these 34-atom units is emphasized, and typical experimental site preferences are indicated.

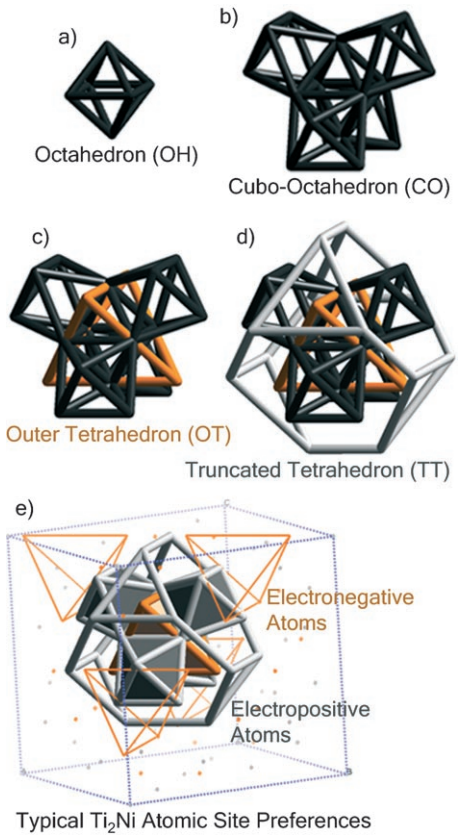

Figure 3. The Ti_2Ni cluster, viewed as four nested polyhedra: a) an octahedron, b) a cubo-octahedron that forms octahedra sharing faces with the central octahedron, c) an outer tetrahedron, and d) a truncated tetrahedron. e) The cluster is also shown in the Ti_2Ni structure itself.

[2] This is a cubo-octahedron in name only. It is very distorted, and can be more accurately described as the outer layer of a pyrochlore unit.[25]

The fourth and final cluster in $Mg_{44}Rh_7$ will here be described as a 16-atom face-centered cubic unit. This cluster, shown in Figure 4, can be viewed in two ways. First, it can

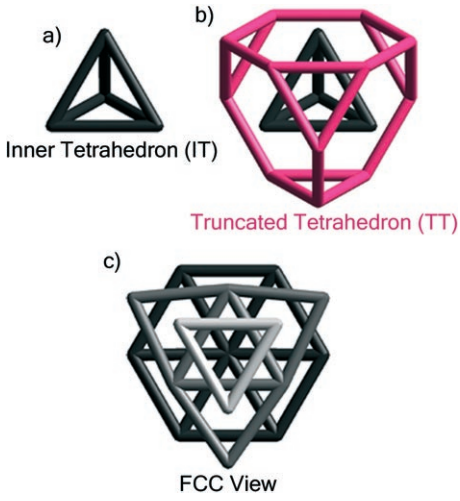

Figure 4. The face-centered cubic cluster, first viewed as nested polyhedra: a) an inner tetrahedron and b) a truncated tetrahedron. c) Alternatively, the atoms are shown in cubic close-packed layers.

be seen as an inner tetrahedron (IT) and a truncated tetrahedron (TT), as in Figure 4a,b. Alternatively, as in Figure 4c, the cluster can be viewed as parts of three layers of cubic closest packing. Because all atoms in a true face-centered cubic structure are crystallographically equivalent, the cluster concept does not allow us to predict the relative electronegativities of the two different sites, IT and TT.

These four distinct clusters, when placed at the high-symmetry points of the $Mg_{44}Rh_7$ unit cell, give a full atomistic description of the structure. Each of the fourteen crystallographically inequivalent sites in $Mg_{44}Rh_7$ lies at a distinct site in one of these clusters.

Site preferences in $Mg_{44}Rh_7$: Based on typical site preferences in the separate γ-brass, Ti_2Ni, and face-centered cubic structures, one can partially rationalize which sites in $Mg_{44}Rh_7$ are likely to be occupied by Mg and Rh. Because Rh (2.28 on the Pauling electronegativity scale) is significantly more electronegative than Mg (1.31), one expects Rh atoms to occupy some combination of the OT and OH sites of the γ-brass clusters (see Figure 2) and the OT site of the Ti_2Ni cluster (see Figure 3), the electronegative sites of these two structure archetypes. The left half of Figure 5 indicates that this prediction is fairly accurate. Of the fourteen

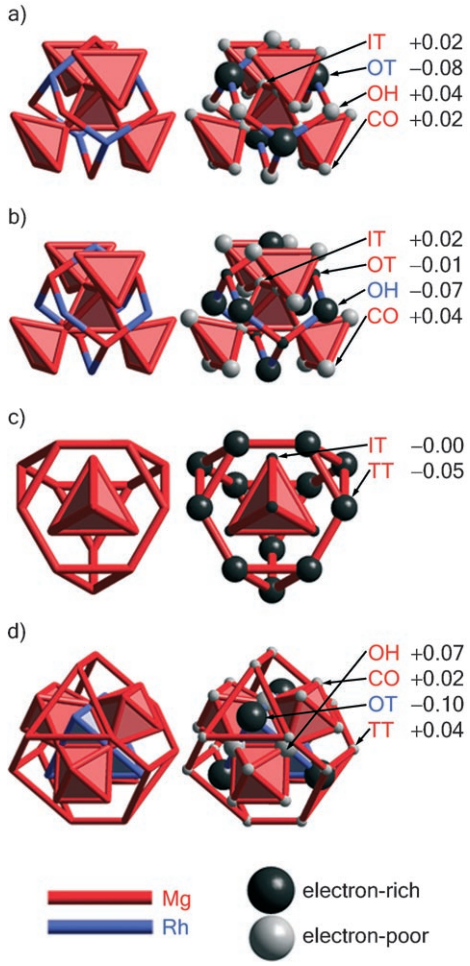

Figure 5. On the left, site placements in the four clusters of $Mg_{44}Rh_7$: a) γ-brass cluster 1 (γ1), b) γ-brass cluster 2 (γ2), c) FCC cluster, d) Ti_2Ni cluster. The three Rh sites in the structure are γ1-OT, γ2-OH, and Ti_2Ni-OT. On the right, Mulliken populations for the homoatomic eH calculation of $Mg_{44}Rh_7$. Charges of greater magnitude are represented by larger spheres. The three most electron-rich sites are occupied by Rh, the more electronegative element.

crystallographically distinct sites in $Mg_{44}Rh_7$, eleven are occupied by Mg atoms (red vertices), and three by Rh (blue vertices). The three Rh sites are the OT site of γ-brass cluster 1 (γ1-OT[3]), the OH site of γ-brass cluster 2 (γ2-OH), and the OT site of the Ti_2Ni cluster (Ti_2Ni-OT).

Although these site preferences are not entirely surprising, they at the same time show the limitations of the cluster model. The cluster model makes no distinction between the OT and OH sites of the two different γ-brass clusters. It therefore does not explain why the OT site of one γ-brass cluster and the OH site of the other are occupied by Rh.

A quantum mechanically guided description of $Mg_{44}Rh_7$, as we will see, need not have this limitation. To lead us toward understanding the site preferences and constructing such a quantum mechanical description, we use Mulliken populations based on simple electronic structure calculations.

The procedure used to calculate Mulliken populations of the fourteen sites in $Mg_{44}Rh_7$ is given in the Computational Methods section of this paper. The results of this calculation are shown in the right half of Figure 5. Black and white spheres, their radii scaling with the magnitudes of the charges, are used to represent electron-rich and electron-poor sites. We note two key results of this calculation. First, the three most electron-rich sites are the three sites occupied by Rh atoms. This is expected, as Rh is the more electronegative element. Therefore, extended Hückel Mulliken populations agree with the experimentally known site preferences. The second result is more surprising. The Mulliken populations tell us that after the three Rh sites, the next most electron-rich site is the TT site of the face-centered cubic cluster (FCC-TT), which is occupied by Mg. Based on the cluster concept described earlier, we might have expected the remaining OT and OH sites in the γ-brass clusters (γ2-OT and γ1-OH) to be more electron-rich. However, after the three Rh sites, the FCC-TT site is the next most electron-rich by a significant margin.

The Mulliken populations suggest that there are features of $Mg_{44}Rh_7$ which the cluster concept alone cannot explain. At the heart of our problem, we must devise a description that differentiates the γ1-OT and γ2-OH sites, which are quite electron-rich and occupied by Rh, from the γ2-OT and γ1-OH sites, which are less electron-rich and occupied by Mg. Also, our description must explain why the FCC-TT site is as electron-rich as it is. From this point forward, we use these facts to help us build upon the cluster view, and guide us toward a more telling description of the $Mg_{44}Rh_7$ structure. In doing so, we will show how some interesting geometric features arise naturally from an elaborate twinning network of the clusters.

Searching for less obvious clusters: The previous results are tantalizing. They suggest that a cluster description can be used to rationalize some, but not all, of the atomic site preferences and Mulliken populations in the $Mg_{44}Rh_7$ structure. We posit that the limitation of the current cluster method is not inherent in the use of clusters, but rather a result of the fact that the clusters considered so far are centered solely at points of high crystallographic symmetry. While visually appealing, there is no reason that high-symmetry clusters are more chemically meaningful than those at other locations in the unit cell. We proceed to examine critically and systematically the $Mg_{44}Rh_7$ structure for clusters similar to those previously described, but which are not located at high-symmetry points.

Which cluster types might we search for? In the case of $Mg_{44}Rh_7$, the natural cluster types are the three already found at high-symmetry points—the γ-brass, Ti_2Ni, and FCC cluster types. As we are to use this cluster analysis to explain site preferences and Mulliken populations, and as the FCC structure is an elemental structure in which all sites are

[3] Here we begin to introduce our own nomenclature for the crystallographic sites in $Mg_{44}Rh_7$. In the Supporting Information, we provide the names of the sites in past literature about the compound.

equivalent, we limit our search to the γ-brass and Ti_2Ni clusters.

We first search the unit cell for γ-brass clusters. As discussed earlier, the innermost layer of a γ-brass cluster (Figure 2a) is the inner tetrahedron. We therefore begin by looking for all distinct tetrahedra in the $Mg_{44}Rh_7$ structure. To ensure that these tetrahedra are nearly regular in geometry, we require that pairs of atoms within a tetrahedron are separated by no more than 3.52 Å—10% longer than the distance between nearest neighbors in elemental Mg. There are 23 distinct tetrahedra in $Mg_{44}Rh_7$ that obey this criterion. We next determine which of these 23 tetrahedra also possess the second layer of the γ-brass cluster, the outer tetrahedron (Figure 2b). The second layer consists of four atoms that cap each face of the inner tetrahedron, forming four more face-sharing tetrahedra. We therefore look for candidates with four face-sharing tetrahedra (again with contacts no longer than 3.52 Å) around the inner tetrahedron.

Table 1. γ-Brass clusters in the $Mg_{44}Rh_7$ structure.

Atoms in tetrahedron (all contacts $\leq$3.52 Å)	# of face-sharing tetrahedra	Complete γ-brass cluster?	Identity
γ1-IT,IT,IT,IT	4	Yes	γ-brass cluster 1
γ2-IT,IT,IT,IT	4	Yes	γ-brass cluster 2
γ1-IT,IT,IT,OT	4	No	
γ1-IT,IT,OT,OH	4	No	
γ2-IT,IT,IT,OT	4	No	
γ2-IT,IT,OT,OH	4	No	

As shown in Table 1, only six of the 23 tetrahedra are the centers of the two innermost layers of the γ-brass cluster, the inner and outer tetrahedra. For these six remaining candidates, we continue this process, checking whether the third layer (Figure 2c, the octahedron) and fourth layer (Figure 2d, the cubo-octahedron) of the γ-brass cluster are present. The result is that the only two of these six candidates that contain all four γ-brass sites are the two previously described γ-brass clusters centered at high-symmetry points. The other four candidates, as it turns out, are contained entirely within the outer layers of one of these two high-symmetry γ-brass clusters. This means that, outside of the two conventional γ-brass clusters, the $Mg_{44}Rh_7$ structure does not have even so much as the two innermost shells of a γ-brass cluster elsewhere in the structure.

The search for copies of the Ti_2Ni cluster proves more interesting. Recall that the innermost layer of a Ti_2Ni cluster (Figure 3a) is the octahedron. We therefore begin by searching for all the octahedra in $Mg_{44}Rh_7$. Again, we require that all atoms within an acceptable octahedron are located no more than 3.52 Å from their four nearest neighbors in the octahedron. As indicated by the first column of Table 2, only six such octahedra exist in the $Mg_{44}Rh_7$ structure. We narrow this list further by determining which of these candidates possess the second layer of the Ti_2Ni cluster, the cubo-octahedron (Figure 3b). The second layer consists of twelve atoms that create four octahedra sharing faces of the central octahedron. We therefore look for candidates with four face-sharing octahedra (again with contacts no longer than 3.52 Å) around the central octahedron. This leaves three candidates, as the second column of Table 2 shows. Continuing the examination of these three remaining candidates, we find that all three also possess the third layer (Figure 3c, the outer tetrahedron) and fourth layer (Figure 3d, the truncated tetrahedron) of the Ti_2Ni cluster. One of them (the octahedron consisting of six Ti_2Ni-OH atoms) is simply the conventional Ti_2Ni cluster centered at a high-symmetry point. The other two, which are not centered at high-symmetry points, are new to us and will be discussed further in the next section.

Table 2. Ti_2Ni clusters in the $Mg_{44}Rh_7$ structure.

Atoms in octahedron (all contacts $\leq$3.52 Å)	# of face-sharing octahedra	Complete Ti_2Ni cluster?	Identity
Ti_2Ni-OH,OH,OH,OH,OH,OH	4	Yes	Ti_2Ni cluster
Ti_2Ni-OH,OH,OH,CO,CO,CO	4	Yes	Ti_2Ni twin 1
γ1-CO, Ti_2Ni-OH,CO,CO,TT,TT	4	Yes	Ti_2Ni twin 2
FCC-IT,IT,IT,TT,TT,TT	3		Ti_2Ni partial twin 1
γ2-CO,CO, Ti_2Ni-TT, FCC-IT,TT,TT	3		Ti_2Ni partial twin 2
γ1-OH,CO, γ2-CO, Ti_2Ni-CO,TT, FCC-TT	3		Ti_2Ni partial twin 3

Understanding site preferences: γ1-OT and γ2-OH versus γ2-OT and γ1-OH: In the previous section, it was concluded that, while the $Mg_{44}Rh_7$ structure contains no copies of the γ-brass cluster aside from those centered at high-symmetry points, two additional copies of the Ti_2Ni cluster are present, and could be worth further analysis. Figure 6 shows where these two "twins" of the Ti_2Ni cluster are located with respect to the high-symmetry clusters. In Figure 6a, we begin with several conventional clusters (i.e., clusters centered at high-symmetry points)—one Ti_2Ni cluster, three FCC clusters, and one γ-brass 1 cluster. Figure 6b highlights 34 atoms at the interface of the conventional clusters which, as Figure 6c shows, constitute one of the twins of the Ti_2Ni cluster. Although this set of atoms, which we will refer to as Ti_2Ni twin 1, lacks the true tetrahedral symmetry of the conventional Ti_2Ni cluster, it has all 34 atoms with only minor distortion. Similarly, the bottom half of Figure 6 shows the second type of Ti_2Ni twin, which we will refer to as Ti_2Ni twin 2. At the interface of one conventional Ti_2Ni, two FCC, two γ-brass 1, and one γ-brass 2 cluster (Figure 6d), another group of 34 atoms (Figure 6e) is shown to be a twin of the Ti_2Ni cluster (Figure 6f).

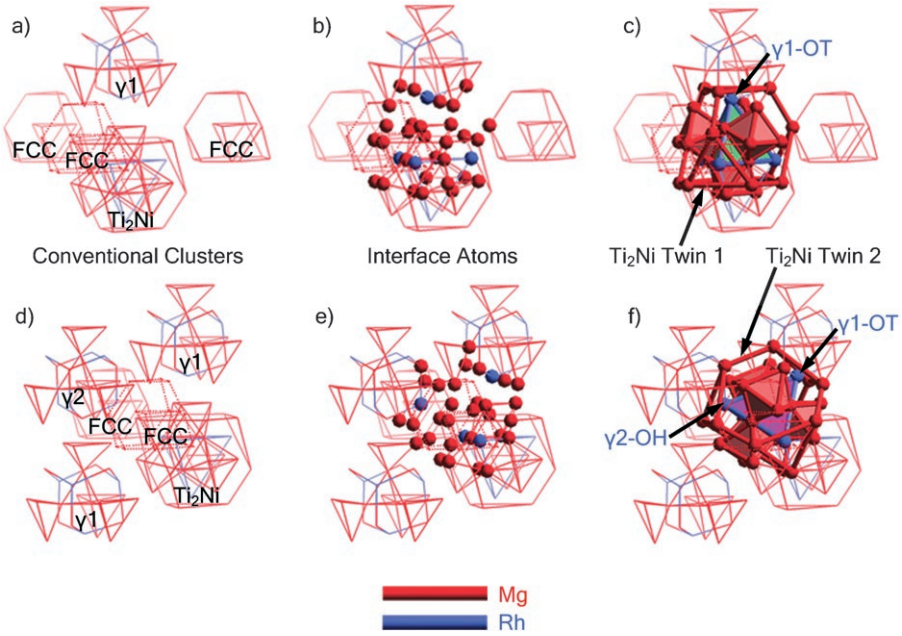

Figure 6. Two types of twins of the Ti_2Ni cluster, constructed at the interfaces of the conventional clusters. a,d) Conventional clusters are centered at high-symmetry points in the crystal. b,e) Thirty-four atoms at the conventional cluster interfaces c,f) are connected to form Ti_2Ni twins.

Taken alone, the observation of twins of the Ti_2Ni cluster is nothing more than a geometric curiosity. However, when considered along with the experimental Mg versus Rh site preferences, the twins take on a more fundamental role in describing the electronic structure of $Mg_{44}Rh_7$. As it turns out, we may use the original Ti_2Ni cluster and its twins to account for the Mg versus Rh site preferences in $Mg_{44}Rh_7$—in particular, to sort out the mystery of why Rh atoms occupy different sites in the two γ-brass clusters.

Without even considering the symmetry of $Mg_{44}Rh_7$ or the names of the various crystallographic sites, one can look at the Ti_2Ni cluster (Figure 5d) and twins (Figure 6c,f), and see that they have strong similarities. In all three 34-atom units, there are exactly four Rh atoms, and they occupy the four positions on the outer tetrahedron. These are exactly the positions at which we would expect electronegative atoms to be found, based on known compounds with the Ti_2Ni structure (see Figure 3). However, because the Ti_2Ni fragments are crystallographically inequivalent, the Rh atoms on their outer tetrahedra have different crystallographic names. In the high-symmetry Ti_2Ni cluster, the four Rh atoms are all located at Ti_2Ni-OT positions. In Ti_2Ni twin 1 (Figure 6c), they occupy three Ti_2Ni-OT positions and one γ1-OT position. In Ti_2Ni twin 2 (Figure 6f), they occupy two Ti_2Ni-OT positions, one γ1-OT position and one γ2-OH position.

Thus, the tendency of electronegative Rh atoms to occupy the positions on the outer tetrahedra of Ti_2Ni clusters and twins explains why they are present at the γ1-OT and γ2-OH sites, and not at the γ2-OT and γ1-OH sites. Rather than seeing the three Rh sites in $Mg_{44}Rh_7$ as a hodgepodge of positions on different clusters, it is therefore less mysterious to view them as the positions on the outer tetrahedron of each occurrence of a Ti_2Ni cluster or twin.

Rationalizing Mulliken populations—the FCC-TT site: That the Ti_2Ni cluster and twins successfully account for the Mg versus Rh site preferences in $Mg_{44}Rh_7$ is most encouraging. But it still does not answer the question of why FCC-TT is the most electron-rich of the Mg sites. This question can be addressed by taking our twinning picture one step farther, and noting that the $Mg_{44}Rh_7$ structure contains yet more fragments of Ti_2Ni. Recall from Table 2 that, in addition to the octahedra at the centers of the high-symmetry Ti_2Ni cluster and its two twins, there are three more types of octahedra in the $Mg_{44}Rh_7$ structure. As it turns out, each of these three octahedra forms the center of a 25-atom partial twin of the Ti_2Ni cluster, illustrated in Figure 7. Each of these partial twins is missing nine atoms from the conventional cluster—three from the cubo-octahedron and six from the truncated

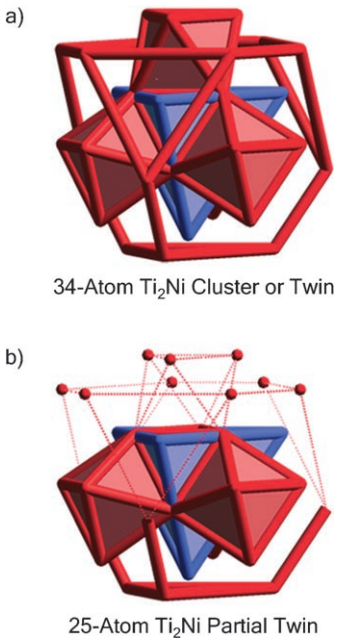

Figure 7. The atoms that comprise the Ti_2Ni partial twins in $Mg_{44}Rh_7$. As compared to a) the Ti_2Ni cluster and twins previously discussed, b) the Ti_2Ni partial twins lack nine atoms (three from the cubo-octahedron and six from the truncated tetrahedron) that are significantly displaced from their original positions.

tetrahedron—which are highlighted in Figure 7b. Unlike the partial γ-brass clusters that were excluded from consideration earlier in this paper, these partial Ti_2Ni twins do not reside within the previously established Ti_2Ni cluster or twins.

The placements of these three types of Ti_2Ni partial twins within the $Mg_{44}Rh_7$ structure are shown in Figure 8. Once

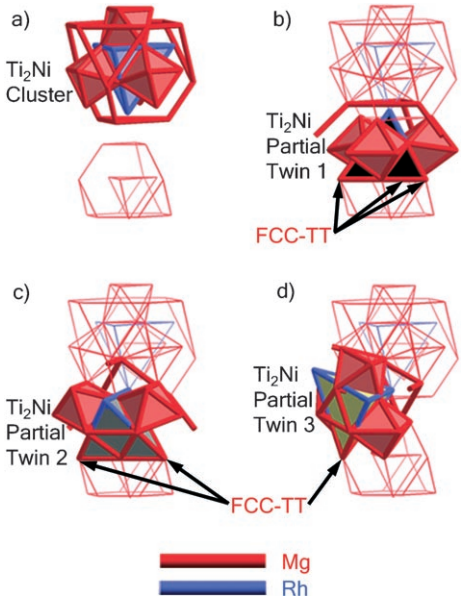

Figure 8. Three types of partial twins of the Ti_2Ni cluster, constructed at the interfaces of the conventional clusters. a) Conventional clusters are centered at high-symmetry points in the crystal. b,c,d) Twenty-five atoms at the conventional cluster interfaces are connected to form Ti_2Ni partial twins.

again, their importance becomes apparent when one notes which sites are on their outer tetrahedra. In Ti_2Ni partial twin 1 (Figure 8b), the outer tetrahedron consists of one Rh atom at a Ti_2Ni-OT position and three Mg atoms at FCC-TT positions (recall that the FCC-TT site is by Mulliken population the most electron-rich Mg site). In partial twin 2 (Figure 8c), the outer tetrahedron consists of one Rh atom at a Ti_2Ni-OT position, a second Rh atom at a γ2-OH position, and two Mg atoms at FCC-TT positions. Finally, in partial twin 3 (Figure 8d), the outer tetrahedron consists of one Rh atom at a Ti_2Ni-OT position, a second Rh atom at a γ1-OT position, a third Rh atom at a γ2-OH position, and one Mg atom at a FCC-TT position.

To sum up, each of the three types of Ti_2Ni partial twins have outer tetrahedra consisting of some combination of the three Rh sites and the single most electron-rich Mg site—the FCC-TT site. This suggests why in our eH electronic structure calculations, FCC-TT was the most electron-rich of the eleven Mg sites in $Mg_{44}Rh_7$. This result can now be explained by the observation that the FCC-TT site lies on the outer tetrahedra of all three types of Ti_2Ni partial twins. To put it another way, *because the FCC-TT site has an environment similar to that of the three Rh sites once we allow ourselves to see the partial twins, it is not surprising that the FCC-TT site is nearly as electron-rich as the Rh sites.*

The twinning of Ti_2Ni clusters appears to correlate with the electron-richness of the various crystallographic sites in $Mg_{44}Rh_7$. In Table 3, we further demonstrate this correlation by showing how the Mulliken population of an atom varies with the number of Ti_2Ni fragments in which it appears on the outer tetrahedron. We see that the larger the number of ways an atom can be shown on the outer tetrahedron of a Ti_2Ni unit, the more electron-rich that atom is in our electronic structure calculations.

Table 3. Ranking the Mulliken populations.

Site	Atom type	Mulliken population	Number of appearances on outer tetrahedron of Ti_2Ni fragment per atom
Ti_2Ni-OT	Rh	−0.10	20
γ1-OT	Rh	−0.08	10
γ2-OH	Rh	−0.07	8
FCC-TT	Mg	−0.05	5
γ2-OT	Mg	−0.01	0
FCC-IT	Mg	−0.00	0
γ1-IT	Mg	+0.02	0
γ1-CO	Mg	+0.02	0
γ2-IT	Mg	+0.02	0
Ti_2Ni-CO	Mg	+0.02	0
γ1-OH	Mg	+0.04	0
γ2-CO	Mg	+0.04	0
Ti_2Ni-TT	Mg	+0.04	0
Ti_2Ni-OH	Mg	+0.07	0

Fivefold symmetry and the edge-capped stella quadrangula: In the previous section, we found that the four most electron-rich sites in the $Mg_{44}Rh_7$ structure all lie on electron-rich positions of the Ti_2Ni fragments. This modified cluster view successfully accounts for the site preferences and the ordering of Mulliken populations in $Mg_{44}Rh_7$. Nonetheless, there are some potentially troubling aspects of this cluster picture. Perhaps the most troubling aspect of our current description is its complete focus on individual Ti_2Ni fragments, rather than the interplay among them. We have yet to describe how the Ti_2Ni pieces fit together within the larger crystal structure. And yet, the interplay among the various Ti_2Ni fragments must have important consequences to the structure. For example, as we have already seen, each atom at the most electron-rich site in the $Mg_{44}Rh_7$ structure (Ti_2Ni-OT) sits simultaneously on 20 Ti_2Ni pieces. Not only do Ti_2Ni fragments lie near each other, they in fact overlap with one another in what seems at first a structurally complex manner.

In this section, we begin to explore the structural interplay among the Ti_2Ni fragments in $Mg_{44}Rh_7$. We will focus our attention on just the core region of each Ti_2Ni piece. In this manner, we will find components that do not overlap spatially, but instead share faces, edges, and vertices with one another. As such sharings are familiar to solid-state chemists, the juxtaposition of the Ti_2Ni fragments becomes much easier to visualize.

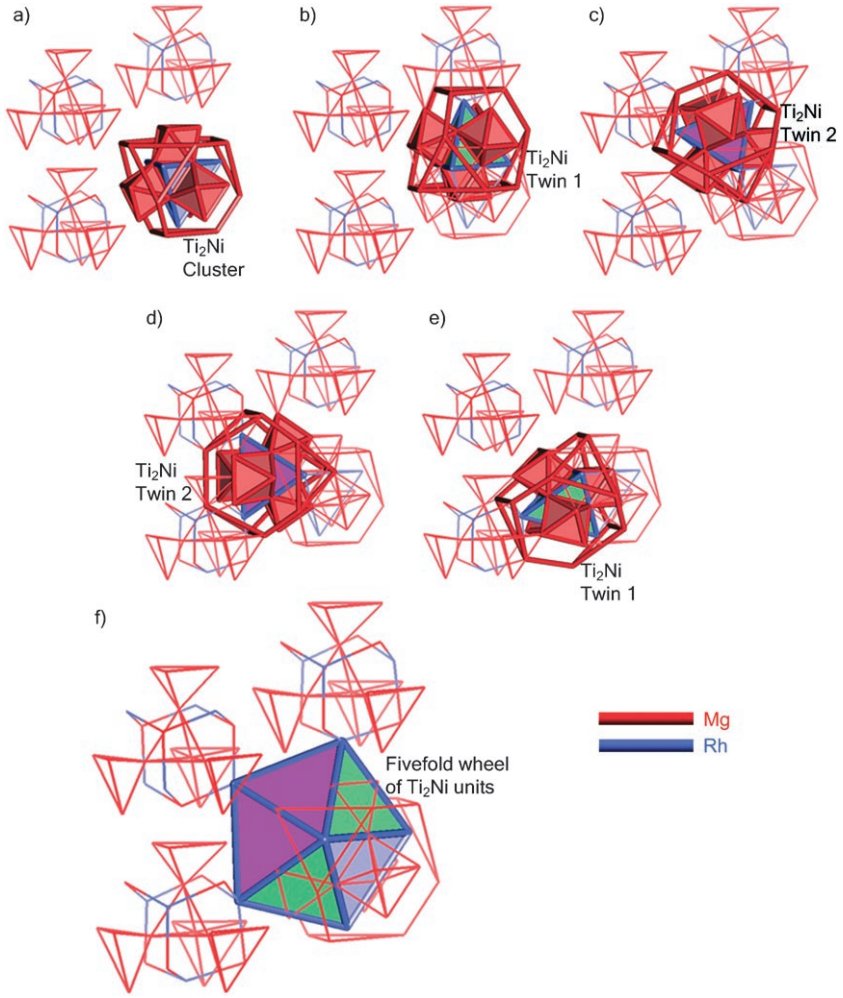

Figure 9. Six views of the same region of the $Mg_{44}Rh_7$ structure: a) the conventional cluster view, b,c,d,e) four views showing twins of the Ti_2Ni cluster at the interfaces of the conventional clusters, and f) a view emphasizing the fivefold symmetry that accompanies this twinning of the Ti_2Ni cluster.

We begin our simplified description in Figure 9, directing much of our focus to the electron-rich outer tetrahedron of each Ti_2Ni piece. Each panel of this figure covers the same region in the $Mg_{44}Rh_7$ structure, but emphasizes a particular feature of the structure. Panels in Figure 9a–e emphasize different individual 34-atom Ti_2Ni clusters or twins in the region. As these pictures show, and as we discussed above, the various Ti_2Ni fragments lie in an overlapping arrangement. Our understanding of the relative placement of these fragments sharpens if we focus just on the outer tetrahedron of each Ti_2Ni piece. Each of these outer tetrahedra consists of four Rh atoms. In Figure 9f, we examine five of these outer tetrahedra, represented as opaque blue, green, and purple units. (Each color of tetrahedron represents a crystallographically distinct Ti_2Ni cluster or twin, consistent with the first five panels of the figure.) These five outer tetrahedra share faces, edges, and vertices with one another, but unlike the full Ti_2Ni pieces, do not overlap in space. As Figure 9f shows, the outer tetrahedra take on the appearance of a fivefold wheel. For the sake of clarity, only one fivefold wheel is shown, but there are actually five more crystallographically equivalent interpenetrating wheels sharing the same conventional (blue) Ti_2Ni cluster.

In Figure 10, we extend beyond the fivefold wheels to build an even larger unit consisting of the outer tetrahedra of Ti_2Ni fragments. The previously described fivefold wheel (Figure 10a) is actually part of an icosahedron (Figure 10b). The 20 tetrahedra that comprise this icosahedron[4] (19 of which are slightly distorted) are all outer tetrahedra of the various types of Ti_2Ni clusters, twins, and partial twins (Figure 10c). This is consistent with the fact that each Rh atom at a Ti_2Ni-OT site is part of 20 different Ti_2Ni units (see Table 3). We extend this picture farther in Figure 10d by showing that the icosahedron of Ti_2Ni outer tetrahedra is part of an even larger unit—a formation consisting of four interlocking icosahedra, in which each tetrahedron is the outer tetrahedron of a Ti_2Ni cluster, twin, or partial twin.

Although Figure 10 illustrates how the various outer tetrahedra fit together, it does not yet give us a sense of where the distinct crystallographic sites lie in the $Mg_{44}Rh_7$ structure. In Figure 11, we build this same construction from the center outward, one crystallographic site at a time. We start with the outer tetrahedron of the conventional high-symmetry Ti_2Ni cluster, consisting of four Ti_2Ni-OT atoms (Figure 11a). We cap the four faces of this tetrahedron with Rh atoms at the γ1-OT positions, forming the outer tetrahedra of Ti_2Ni twin 1 (Figure 11b). Next, we cap the edges of the resulting polyhedron with six Rh atoms at the γ2-OH positions, forming the outer tetrahedra of Ti_2Ni twin 2 (Figure 11c). Finally, we cap the edges again with twelve Mg atoms at the FCC-TT positions, forming the outer tetrahedra of all three types of Ti_2Ni partial twins (Figure 11d).

This set of 26 atoms in Figures 10d and 11d is known as an edge-capped stella quadrangula, and has been previously noted for its prevalence in intermetallic and ionic structures.[5] We see here that the outer tetrahedra of the various Ti_2Ni units in $Mg_{44}Rh_7$ form an edge-capped stella quadran-

[4] An icosahedron with an atom in its center can also be viewed as 20 face-sharing tetrahedra.

[5] When Nyman and Andersson introduced the edge-capped stella quadrangula, they suggested that it is the furthest extent to which tetrahedra can be packed in space without severe distortion. They also asserted that the stella quadrangula and its edge-capped variants are important building units in many intermetallic and ionic structures.[27,28]

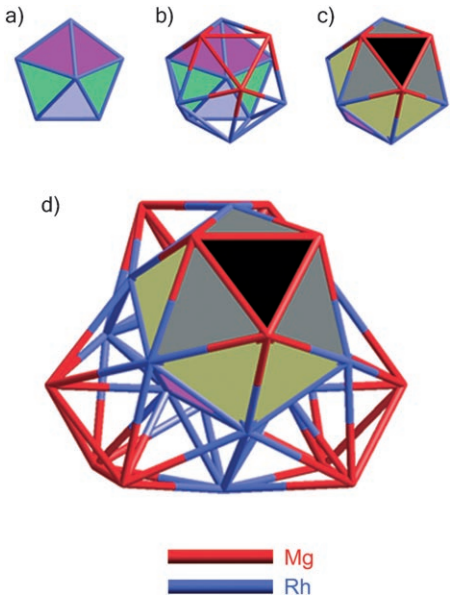

Figure 10. Larger features of fivefold symmetry in the $Mg_{44}Rh_7$ structure. a) The fivefold wheel of outer tetrahedra of Ti_2Ni fragments is part of b,c) an icosahedron of such outer tetrahedra. This icosahedron is in turn part of d) a formation of four interlocking icosahedra.

The electronic basis of the stella quadrangula model: In the left half of Figure 12, we again build the edge-capped stella quadrangula from center outward, this time showing all the atoms in the vicinity, rather than just those on the outer tetrahedra of Ti_2Ni fragments. The newly introduced atoms, all of which are Mg and are represented by red balls, are located at roughly the center of each edge of this construction.

We now come to an important point. As shown in the right half of Figure 12, the atoms on the vertices and those on the edges differ *electronically*. The atoms on the vertices of the edge-capped stella quadrangula (i.e., those on the outer tetrahedra of Ti_2Ni fragments) are electron-rich, while the atoms on the edges are electron-poor or neutral.

This construction therefore illustrates a potentially chemically significant order in the $Mg_{44}Rh_7$ structure. Rather than describing the structure as a hodgepodge of clusters in which site preferences and Mulliken populations are somewhat mysterious, we now describe it in terms of a single building block from which the site preferences and relative Mulliken populations follow naturally. We now see an edge-capped stella quadrangula in which electron-rich atoms occupy the vertices, and electron-poor or neutral atoms lie at the center of each edge.

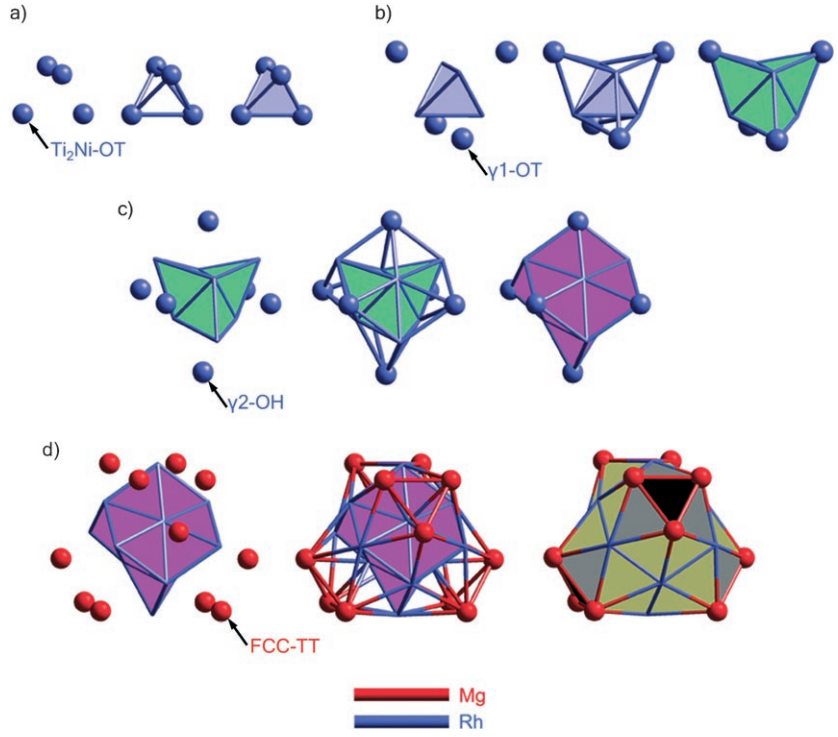

Figure 11. An alternate way to build up the interlocking icosahedra, this time from center outward. a,b,c,d) The outer tetrahedra of the various Ti_2Ni fragments are placed face-to-face to form the same 26-atom arrangement as shown earlier.

Surprising features of $Mg_{44}Rh_7$: Our description of $Mg_{44}Rh_7$ highlights some remarkable features of the structure. One such feature is the presence of the same repeating motif—the edge-capped stella quadrangula—on different length scales within $Mg_{44}Rh_7$. The edge-capped stella quadrangula is identical to a grouping we introduced early in this paper, but referred to by a different name. As shown in Figure 13, *the 26-atom edge-capped stella quadrangula is fully equivalent to the 26-atom γ-brass cluster*. However, there is an important difference between the γ-brass clusters we described in Figure 2 and the edge-capped stella quadrangula we introduced in Figure 10. The γ-brass clusters occur on roughly the length scale of the chemical bond (nearest neighbors lie between 2.69 and 3.88 Å apart), and include all atoms within a given region of the $Mg_{44}Rh_7$ structure. The edge-capped stella quadrangula we introduced in Figure 10, however, is on a longer length scale (nearest neighbors lie between 5.56 and 6.43 Å apart), and does not include all atoms in the region. It includes only the most electron-rich

gula. As demonstrated in Figure 12 by Mulliken populations, this edge-capped stella quadrangula proves to be the essential unit not just in locating the electron-rich atoms on the outer tetrahedra of Ti_2Ni pieces, but in understanding all the crystallographic sites in the $Mg_{44}Rh_7$ structure.

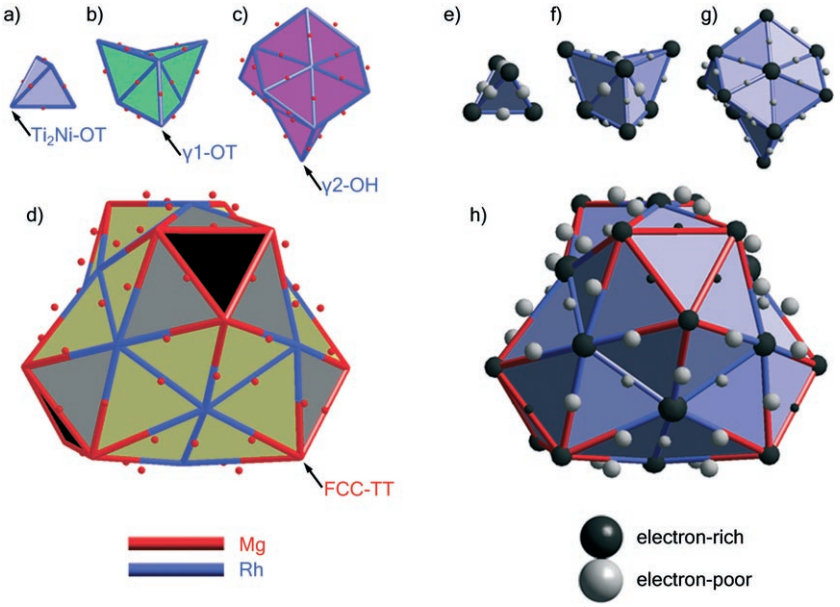

Figure 12. Site preferences and Mulliken populations within the edge-capped stella quadrangula. a,b,c,d) The edge-capped stella quadrangula is again built in layers, this time with Mg atoms at the center of each edge. e,f,g,h) Mulliken populations show that electron-rich atoms occupy the vertices, while electron-poor or neutral atoms occupy the edge-centers.

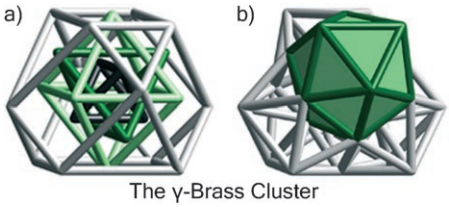

Figure 13. Two views of the 26-atom γ-brass cluster. The cluster can be described a) as nested polyhedra or b) as an edge-capped stella quadrangula, consisting of four interlocking icosahedra.

atoms in the $Mg_{44}Rh_7$ structure—the three Rh sites, and the most electron-rich Mg site.

This suggests a fractal-like hierarchy in the $Mg_{44}Rh_7$ structure. At the length scale of chemical bonds, atoms arrange themselves in 26-atom γ-brass clusters, which are equivalent to edge-capped stellae quadrangulae. Meanwhile, the most electron-rich atoms in the structure fix their positions at the vertices of larger 26-atom edge-capped stellae quadrangulae. All of these polyhedra on different length scales interpenetrate to form the intricate $Mg_{44}Rh_7$ structure that nature so cleverly devised.

The second remarkable feature of $Mg_{44}Rh_7$ is the prevalence of fivefold symmetry in its diffraction pattern. As illustrated throughout this paper, and previously by Samson and Hansen,[6] the $Mg_{44}Rh_7$ structure is filled with features of approximate fivefold symmetry, in the form of fivefold wheels, icosahedra, and edge-capped stellae quadrangulae. The structure as a whole also exhibits a push toward fivefold symmetry, which manifests itself not only in the crystallographic geometry, but also in a striking way in reciprocal space. Note the approximate fivefold symmetry in the simulated single-crystal diffraction pattern of $Mg_{44}Rh_7$ in the [1 1 0] direction,[29] shown in Figure 14.

Interestingly, the fivefold symmetry in $Mg_{44}Rh_7$ is along the $\langle 1\,1\,0\rangle$ directions, rather than the $\langle 1\,\tau\,0\rangle$ directions more commonly associated with quasicrystalline approximants.[30] Although the apparent fivefold symmetry in $Mg_{44}Rh_7$ cannot be true crystallographic symmetry, the diffraction pattern can apparently approach fivefold symmetry as a limit as fivefold formations within the structure become increasingly decorated. This approximate fivefold symmetry could well be an essential part of the stability of the compound.

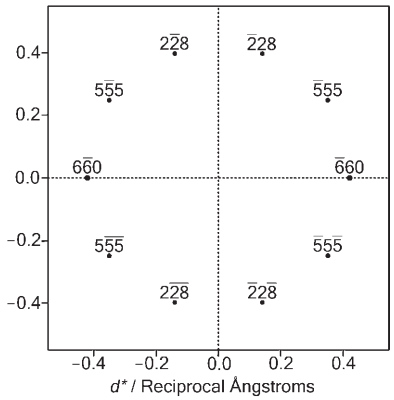

Figure 14. Simulated single-crystal X-ray diffraction pattern of $Mg_{44}Rh_7$, viewed in the [1 1 0] direction. Only the ten brightest peaks are shown. We provide a more complete list of peaks in the Supporting Information.

Conclusion

We have presented a new description of the $Mg_{44}Rh_7$ structure. There are several features of our lengthy description that we believe are worth noting. First, the computational methods used in this paper are simple enough to allow for calculations of even the largest known intermetallic and ionic crystal structures, which have upwards of one thousand atoms per unit cell. But perhaps more importantly, our approach suggests a general way in which large intermetallic structures can be understood. As long as one chooses an appropriate cluster to search for, our approach can be generalized to a wide variety of structures. The search algorithm we employed, which checks the entire unit cell for copies of a

given atomic arrangement, is an unbiased way to locate a given geometric feature.

The concept of identifying important building units and searching for them in a structure is already deeply ingrained in the minds of chemists. When organic chemists view molecules, their eyes are drawn to familiar motifs such as aromatic rings and cyclohexane rings, from which they have come to expect certain chemical behaviors. The approach in this paper is predicated on this same idea of systematically searching for familiar (and in our case, fundamentally intermetallic) chemical units, such as the 26-atom γ-brass cluster or the 34-atom Ti_2Ni cluster, to explore an unfamiliar crystal structure.

The concept of viewing a solid-state structure as a combination of overlapping atomic clusters (as in Figures 6, 8, and 9) is also one with a parallel in organic chemistry—namely, resonance. When organic chemists invoke resonance, they draw multiple configurations of two-electron bonds, because just one configuration cannot satisfactorily describe the electronic structure. Likewise, we highlight multiple copies of overlapping clusters,[6] because just one cluster cannot account for all site preferences and Mulliken populations in $Mg_{44}Rh_7$. Our observation, that the most electron-rich sites in $Mg_{44}Rh_7$ are those that appear on the outer tetrahedra of the most Ti_2Ni fragments, is equivalent to saying the most electron-rich atoms are those that lie at electron-rich positions in the greatest number of resonance structures.

Because we use electronic structure calculations as a guide, the goal of our approach is to uncover geometric features that are more likely to be of chemical importance to the compound. These features—notably the fractal-like structure with edge-capped stellae quadrangulae on different length scales, and the approximate fivefold symmetry of the ⟨110⟩ single-crystal diffraction patterns—are present in many other complicated intermetallic and ionic structures. Only by cataloguing these and similar features in a variety of structures can we hope to explore the open question of what drives such complex crystal structures to exist.

Computational Methods

We used LDA-DFT-calibrated extended Hückel (eH) calculations to derive the experimentally known Mg versus Rh site preferences in $Mg_{44}Rh_7$. Using the same "generic" atomic parameters at all atomic sites in $Mg_{44}Rh_7$, Mulliken populations were calculated, and the more electronegative Rh atoms were assumed to prefer sites with larger Mulliken populations. This assumption has been successfully employed to derive intermetallic site preferences many times in the past.[24,32–36] Before Mulliken populations could be calculated, atomic parameters for the eH calculation of $Mg_{44}Rh_7$ were calibrated against LDA-DFT calculations to ensure that they were physically reasonable.

As a first step in the parameter calibration process, a "parent compound" was selected—one with a somewhat similar stoichiometry and structure to the compound of interest, but with a unit cell small enough to allow LDA-DFT calculations. In this case, a reasonable choice was Mg_5Rh_2, which crystallizes in hexagonal space group $P6_3/mmc$ (No. 194).

[6] When dealing with solid-state structures, one who applies this technique is often said to wear "Schnering's spectacles."[31]

Next, the LDA-DFT band structure of the parent compound Mg_5Rh_2 was calculated using the VASP package[37–40] with ultra-soft Vanderbilt pseudopotentials.[41] Starting with the experimentally determined crystal structure of Mg_5Rh_2,[42] unit-cell dimensions and atomic positions were optimized by using a $3\times3\times3$ Monkhorst-Pack k-point mesh.[43] Charge density was then calculated by using a $5\times5\times5$ Monkhorst-Pack k-point mesh. Finally, the LDA-DFT band structure of Mg_5Rh_2 shown in Figure 15a was calculated k-point by k-point, using the previously determined charge density.

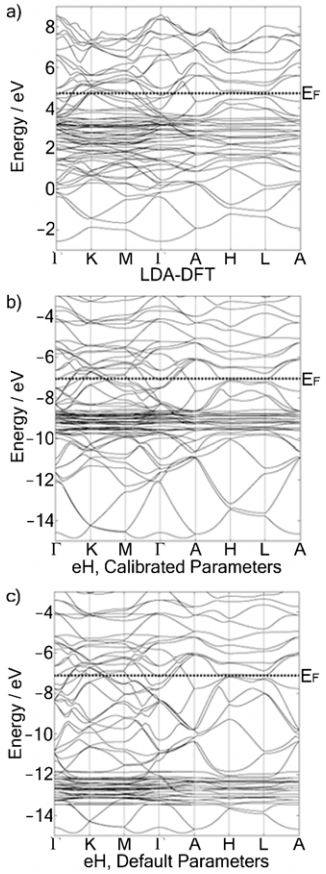

Figure 15. Band structures of Mg_5Rh_2 near the Fermi energy, calculated using a) LDA-DFT methods, b) extended Hückel methods with atomic parameters calibrated to mimic the LDA-DFT band structure, and c) extended Hückel methods with default Mg and Rh parameters. $\Gamma=(0,0,0)$, $K=(-\frac{1}{3},\frac{2}{3},0)$, $M=(0,\frac{1}{2},0)$, $A=(0,0,\frac{1}{2})$, $H=(-\frac{1}{3},\frac{2}{3},\frac{1}{2})$, and $L=(0,\frac{1}{2},\frac{1}{2})$.

After this LDA-DFT band structure was calculated, eH atomic parameters of Mg and Rh were adjusted until they generated an eH band structure of Mg_5Rh_2 with features similar to the LDA-DFT band structure. All eH calculations were carried out with the YAeHMOP package,[44] by using experimentally determined crystal structures rather than theoretically optimized geometries. The eH atomic parameters that provided the closest match to the LDA-DFT band structure were: H_{ii}(Mg 3s) = −9.0 eV, $\zeta_s=1.1$; H_{ii}(Mg 3p) = −4.5 eV, $\zeta_p=1.1$; H_{ii}(Rh 5s) = −8.09 eV, $\zeta_s=2.135$; H_{ii}(Rh 5p) = −4.57 eV, $\zeta_p=2.1$; H_{ii}(Rh 4d) = −9.0 eV, $\zeta1_d=4.29$, $\zeta2_d=1.70$, $c1_d=0.5807$, $c2_d=0.5685$. Figure 15b shows the eH band structure generated by using these calibrated parameters, while Figure 15c shows the eH band structure generated using default parameters.[45]

As the pictures suggest, raising the Rh 4d orbital energies from H_{ii}(Rh 4d) = −12.5 eV to H_{ii}(Rh 4d) = −9.0 eV substantially improves the fit

between eH and LDA-DFT calculations. Aside from this adjustment of the Rh 4d orbital energies, all other eH default atomic parameters seemed reasonable. While not identical to the LDA-DFT band structure, the calibrated eH band structure mimics many of the LDA-DFT features, especially near the Fermi energy. Such calibration methods have proven reliable in the past.[24,36,46–48]

Using our newly calibrated eH atomic parameters, Mulliken populations were calculated for the structure of interest, $Mg_{44}Rh_7$. All atomic sites were given Mg parameters (the majority element), so as not to bias the calculation toward the experimentally known site preferences. Mulliken populations were averaged over 60 uniformly distributed *k-p*oints in the ($k_x > 0$, $k_y > 0$, $k_z > 0$, $k_x \geq k_y \geq k_z$) portion of the first Brillouin zone.

Acknowledgements

This research was supported by the National Science Foundation (through grant DMR-0504703). We thank Daniel C. Fredrickson for pointing out to us the similarity of the cluster view in intermetallic systems to resonance structures in organic chemistry.

[1] S. Samson, *Nature* **1962**, *195*, 259–262.
[2] S. Samson, *Acta Crystallogr.* **1965**, *19*, 401–413.
[3] S. Samson, *Acta Crystallogr.* **1967**, *23*, 586–600.
[4] P. Villars, L. Calvert, *Pearson's Handbook of Crystallographic Data for Intermetallic Phases*, 2nd ed., ASM International: Materials Park, OH, **1967**.
[5] L. Westin, *Chem. Scr.* **1971**, *1*, 127–135.
[6] S. Samson, D. Hansen, *Acta Crystallogr. Sect. B* **1972**, *28*, 930–935.
[7] S. Andersson, *Acta Crystallogr. Sect. A* **1978**, *34*, 833–835.
[8] A. Bradley, P. Jones, *J. Inst. Met.* **1933**, *51*, 131–162.
[9] B. Chabot, K. Cenzual, E. Parthé, *Acta Crystallogr. Sect. A* **1981**, *37*, 6–11.
[10] W. Hornfeck, S. Thimmaiah, S. Lee, B. Harbrecht, *Chem. Eur. J.* **2004**, *10*, 4616–4626.
[11] A. Zalkin, W. Ramsey, *J. Phys. Chem.* **1958**, *62*, 689–693.
[12] S. Samson, *Acta Crystallogr. Sect. B* **1972**, *28*, 936–945.
[13] M. Booth, J. Brandon, R. Brizard, C. Chieh, W. Pearson, *Acta Crystallogr. Sect. B* **1977**, *33*, 30–36.
[14] M. Fornasini, B. Chabot, E. Parthé, *Acta Crystallogr. Sect. B* **1978**, *34*, 2093–2099.
[15] A. Koster, J. Schoone, *Acta Crystallogr. Sect. B* **1981**, *37*, 1905–1907.
[16] R. Nesper, H.-G. von Schnering, *J. Solid State Chem.* **1987**, *70*, 48–57.
[17] S. Lidin, M. Jacob, A.-K. Larsson, *Acta Crystallogr. Sect. C* **1994**, *50*, 340–342.
[18] S. Mahne, B. Harbrecht, *J. Alloys Compd.* **1994**, *203*, 271–279.
[19] F. Bonhomme, K. Yvon, *J. Alloys Compd.* **1995**, *227*, L1L3.
[20] T. Nasch, W. Jeitschko, *J. Solid State Chem.* **1999**, *143*, 95–103.
[21] B. Harbrecht, S. Thimmaiah, M. Armbrüster, C. Pietzonka, S. Lee, *Z. Anorg. Allg. Chem.* **2002**, *628*, 2744–2749.
[22] V. Smetana, V. Babizhetskyy, G. Vajenine, A. Simon, *Angew. Chem.* **2006**, *118*, 6197–6200; *Angew. Chem. Int. Ed.* **2006**, *45*, 6051–6053.
[23] O. von Heidenstam, A. Johansson, S. Westman, *Acta Chem. Scand.* **1968**, *22*, 653–661.
[24] J. Schmidt, S. Lee, D. Fredrickson, *Chem. Eur. J.* **2007**, *13*, 1394–1410.
[25] M. O'Keeffe, B. Hyde, *Crystal Structures I: Patterns and Symmetry*, Mineralogical Society of America, Washington, DC, **1996**.
[26] G. Yurko, J. Barton, J. Parr, *Acta Crystallogr.* **1959**, *12*, 909–911.
[27] H. Nyman, S. Andersson, *Acta Crystallogr. Sect. A* **1979**, *35*, 580–583.
[28] H. Nyman, S. Andersson, *Acta Crystallogr. Sect. A* **1979**, *35*, 934–937.
[29] *Cerius2*, *v. 3.8*, Molecular Simulations, Inc.: San Diego, CA, **1998**.
[30] C. Janot, *Quasicrystals: A Primer*, 2nd ed., Clarendon, Oxford, **1994**.
[31] H. von Schnering, *Angew. Chem.* **1981**, *93*, 44–63; *Angew. Chem. Int. Ed. Engl.* **1981**, *20*, 33–51.
[32] J. Burdett, S. Lee, T. McLarnan, *J. Am. Chem. Soc.* **1985**, *107*, 3083–3089.
[33] J. Burdett, E. Canadell, T. Hughbanks, *J. Am. Chem. Soc.* **1986**, *108*, 3971–3976.
[34] G. Miller, *Eur. J. Inorg. Chem.* **1998**, *5*, 523–536.
[35] C.-S. Lee, G. Miller, *Inorg. Chem.* **2001**, *40*, 338–345.
[36] D. Fredrickson, S. Lee, R. Hoffmann, *Angew. Chem.* **2007**, *119*, 2004–2023; *Angew. Chem. Int. Ed.* **2007**, *46*, 1958–1976.
[37] G. Kresse, J. Hafner, *Phys. Rev. B* **1993**, *47*, 558–561.
[38] G. Kresse, J. Hafner, *Phys. Rev. B* **1994**, *49*, 14251–14269.
[39] G. Kresse, J. Furthmüller, *Comput. Mater. Sci.* **1995**, *6*, 15–50.
[40] G. Kresse, J. Furthmüller, *Phys. Rev. B* **1996**, *54*, 11169–11186.
[41] D. Vanderbilt, *Phys. Rev. B* **1990**, *41*, 7892–7895.
[42] R. Ferro, *Atti Accad. Naz. Lincei Cl. Sci. Fis. Mat. Nat. Rend.* **1960**, *29*, 70–73.
[43] H. Monkhorst, J. Pack, *Phys. Rev. B* **1976**, *13*, 5188–5192.
[44] G. Landrum, "YAeHMOP: Yet Another extended Hückel Molecular Orbital Package, Version 2.0b", YAeHMOP is freely available on the WWW at URL: http://sourceforge.net/projects/yaehmop/.
[45] P. Alemany, S. Alvarez, **1976**, unpublished work cited in an unpublished table of eH parameters compiled by S. Alvarez.
[46] D. Fredrickson, S. Lee, R. Hoffmann, J. Lin, *Inorg. Chem.* **2004**, *43*, 6151–6158.
[47] D. Fredrickson, S. Lee, R. Hoffmann, *Inorg. Chem.* **2004**, *43*, 6159–6167.
[48] P. Clark, S. Lee, D. Fredrickson, *J. Solid State Chem.* **2005**, *178*, 1269–1283.

Received: June 18, 2007
Published online: August 29, 2007

